

A^-) are expected to lead to a high ρ value.

Conclusions

We have described here a theoretical framework which provides some guidelines for designing conducting D-A complexes, and which forms a basis for future studies of specific case. Our conclusions follow.

(a) We propose that for many of the segregated-stacks organic metals there should in principle exist a thermodynamically more or as stable mixed-stacks form. In this, we are in sympathy with the spirit of section 9 in Perlstein's excellent article.^{2a} Thus, to ensure the formation of segregated-stacks materials, for any D-A pair, one must design molecules where the segregation is built in.

(b) The two-dimensionality is one way of stabilizing the conducting isomer which now "feels" some of the interactions of a mixed-stacks isomer.

(c) The value of ρ of the segregated-stacks isomer depends on the combined effects of $I_D - A_A$, and the extent of geometric reorganization of the ions D^+ and A^- . This interplay merits further studies.

(d) This $\rho \neq 0$ state of the segregated-stacks isomer can lie anywhere from an endothermic to an exothermic species with respect to the neutral $\dots D^0 D^0 | A^0 A^0 \dots$ relaxed state. D-A pairs

with $I_D - A_A \geq 4$ eV are expected to be at the limit of thermo-neutrality and may exhibit reversible $\dots D^{+\rho} D^{+\rho} | A^{-\rho} A^{-\rho} \rightarrow \dots D^0 D^0 | A^0 A^0 \dots$ transitions, with a barrier of $\sim 1/4\alpha(\rho)$ (eq 9).

(e) The $\rho \neq 0$ configurations of the segregated-stacks isomer can develop into a band of delocalized charge-transfer states in a manner which resembles the interactions and the level spread in Hückel systems. This treatment can be used to study other similar systems⁹ such as complex salts (e.g., Cs_2TCNQ_3).

(f) The delocalized intermediate valence states of the segregated-stacks isomer, $\dots D^{+\rho} D^{+\rho} | A^{-\rho} A^{-\rho}$, may be less stable than a collection of localized states. This leads to a small barrier for electron hopping (Figure 3a). In the macroscopic stacks, the variants of the elementary instability (Figure 3a) increase. For example, in the $\rho = 0.5$ state, there will be a tendency for localization of dimers (e.g., $\dots A^{-0.5} A^{-0.5} A^0 A^0 \dots$) or of tetramers (e.g., $\dots A^- A^0 A^- A^0 \dots$) etc. Minimization of this barrier can be achieved by selecting D's and A's which can maintain large intra-stack overlap (large β_{DD} and β_{AA}), and whose ionic states D^+ and A^- involve only small geometric reorganization.

Application to specific systems will be treated in future papers.

Acknowledgment. I thank Professors A. Pross and J. Bernstein for their enlightening comments and for sharing my enthusiasm.

Photoelectron Spectroscopic Studies of the Intermolecular Complexes $(CH_3)_2O \cdot HF$ and $(CH_3)_2S \cdot HF$

F. Carnovale, M. K. Livett, and J. B. Peel*

Contribution from the Department of Physical Chemistry and Research Centre for Electron Spectroscopy, La Trobe University, Bundoora, Victoria 3083, Australia.

Received December 28, 1981

Abstract: The He I photoelectron spectra of the gas-phase complexes formed by dimethyl ether and dimethyl sulfide with hydrogen fluoride have been measured by using a pinhole inlet system with high-pressure equilibrium mixtures of the respective gases. Spectra representing each complex in a "pure" form are obtained by a spectrum-stripping procedure which removes the appropriate monomer spectra from each mixed spectrum. The results of molecular orbital calculations show good agreement with the measured ionization potential shifts occurring on complexation. The data show that the intermolecular hydrogen bond stabilizes the nonbonding electrons of n_O in $(CH_3)_2O$ by 1.0 eV and the nonbonding electrons of n_S in $(CH_3)_2S$ by 0.8 eV. This is found to be mainly due to the electrostatic effect of the polar HF moiety which has a greater influence in the stronger complex. By comparison the apparent destabilization of the nonbonding π_F electrons by 1.6 eV in $(CH_3)_2O \cdot HF$ and 1.2 eV in $(CH_3)_2S \cdot HF$ is also influenced by charge transfer and the relaxation effect of electron rearrangement accompanying ionization.

Ultraviolet photoelectron (PE) spectroscopy has recently been applied to the study of gas-phase intermolecular complexes. While relatively strong complexes had been studied earlier by Lloyd and Lynaugh¹ and by Lake² using the normal low vapor pressure regime of the typical PE spectrometer, the study of weaker complexes has required the use of effusive nozzle inlet systems,^{3,4} as well as supersonic molecular beam techniques.⁵

In recent studies in this laboratory the He I spectra of some carboxylic acid dimers^{6,7} and the dimethyl ether-hydrogen chloride

complex⁸ have been measured. The technique used in this latter study has been utilized in obtaining the He I spectra of the related complexes $(CH_3)_2O \cdot HF$ and $(CH_3)_2S \cdot HF$ that are reported in this paper.

The gas-phase heterodimer of $(CH_3)_2O$ and HF has been detected in infrared spectroscopic studies.⁹⁻¹¹ The complex has been found to have a hydrogen bond energy (ΔH) of 43 kJ mol⁻¹, and the intermolecular hydrogen bond vibration has been identified at 170 cm⁻¹. These studies show that higher cluster species other than the 1:1 complex exist in negligible concentrations in mixtures containing an excess of $(CH_3)_2O$.

The same studies have shown indications of hydrogen bonding in mixtures of $(CH_3)_2S$ and HF, though investigation of the complex is less complete.⁹ This is not surprising in view of the

- (1) D. R. Lloyd and N. Lynaugh, *Chem. Commun.*, 1545 (1970).
- (2) R. F. Lake, *Spectrochim. Acta, Part A*, **27A**, 1220 (1971).
- (3) T. H. Gan, J. B. Peel, and G. D. Willett, *J. Chem. Soc., Faraday Trans. 2*, **73**, 1459 (1977).
- (4) K. Nomoto, Y. Achiba, and K. Kimura, *Chem. Phys. Lett.*, **63**, 277, (1979).
- (5) P. M. Dehmer and J. L. Dehmer, *J. Chem. Phys.*, **67**, 1774 (1977); **68**, 3462 (1978); **69**, 125 (1978).
- (6) F. Carnovale, M. K. Livett, and J. B. Peel, *J. Chem. Phys.*, **71**, 255 (1979).
- (7) F. Carnovale, T. H. Gan, and J. B. Peel, *J. Electron Spectrosc. Relat. Phenom.*, **20**, 53 (1980).

- (8) F. Carnovale, M. K. Livett, and J. B. Peel, *J. Am. Chem. Soc.*, **102**, 569 (1980).
- (9) J. Arnold and D. J. Millen, *J. Chem. Soc.*, 503 (1965).
- (10) M. Couzi, J. le Calvé, P. V. Huang, and J. Lascombe, *J. Mol. Struct.*, **5**, 363 (1970).
- (11) R. K. Thomas, *Proc. R. Soc. London, Ser. A*, **322**, 137 (1971).

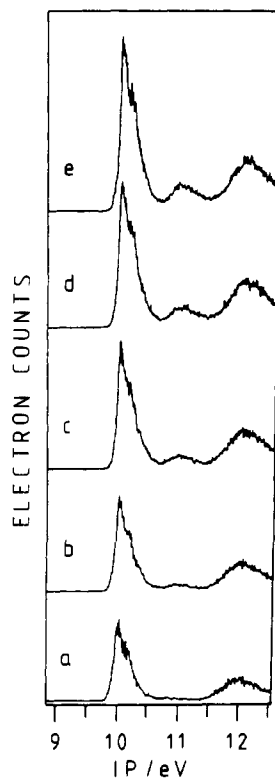


Figure 1. He I photoelectron spectra of a $(\text{CH}_3)_2\text{O}/\text{HF}$ mixture measured with a $50\ \mu\text{m}$ diameter nozzle. The total stagnation pressures (atm) for each are (a) 0.2, (b) 0.3, (c) 0.5, (d) 0.6, and (e) 0.8.

lower association energy expected for this species.

Experimental Section

The computer-controlled ultraviolet PE spectrometer, specially designed for the study of transient molecular species, has been described in detail elsewhere.¹² Whereas glass nozzles of various diameters were used in earlier studies^{3,6-8} of effusive molecular beams, the measurements involving HF were obtained by using a system which consisted of pinholes in thin nickel disks supported in a small cylindrical stainless steel holder fixed to the end of a flexible 6 mm o.d. Teflon tube in which the respective gaseous monomers were mixed.

At room temperature $(\text{CH}_3)_2\text{O}$ has a considerably higher vapor pressure than HF, so the higher pressure mixtures of $(\text{CH}_3)_2\text{O}$ and HF consisted of an excess of $(\text{CH}_3)_2\text{O}$. Several single-sweep He I spectra covering the 9–13-eV ionization potential (IP) range are shown in Figure 1 for a typical $(\text{CH}_3)_2\text{O}\cdot\text{HF}$ mixture. Spectra a–e are of this mixture at stagnation pressures increasing from 0.2 to 0.8 atm. It is clear that the weak band near 11 eV is associated with the increase in pressure, and since it disappears with reduction in the partial pressure of either $(\text{CH}_3)_2\text{O}$ or HF, it is reasonable to assign it as arising from the 1:1 heterodimer $(\text{CH}_3)_2\text{O}\cdot\text{HF}$.

The possible formation of higher clusters was avoided by choosing the mixture depicted in Figure 1d for time averaging. An approximate band intensity analysis suggests that this mixture contains about 14% of complexed $(\text{CH}_3)_2\text{O}$. The time-averaged spectra each of 1024 points are shown in Figure 2. The superimposed spectra of $(\text{CH}_3)_2\text{O}$ and HF in Figure 2a were obtained at similar count rates to those of the 0.6-atm equilibrium mixture of $(\text{CH}_3)_2\text{O}$ and HF shown in Figure 2b. Each time-averaged run was of ~ 2 -h duration and the IP calibration was based on the known monomer IP data.

Other features of the spectrum in Figure 2b which can be attributed to the complex species are not as prominent as the band near 11 eV. However, an increase of intensity near 12.5 eV between the second and third bands of $(\text{CH}_3)_2\text{O}$ as well as a relative increase in intensity of the $(\text{CH}_3)_2\text{O}$ band near 14 eV can be discerned.

A description of the spectrum-stripping procedures used in PE studies of mixtures has been given earlier.⁸ An interactive computer program involving spectrum display facilities has been developed. A measure of its efficacy is the He I spectrum obtained for the very reactive NHBr_2 from a mixture estimated to contain only 2% of this species.¹³

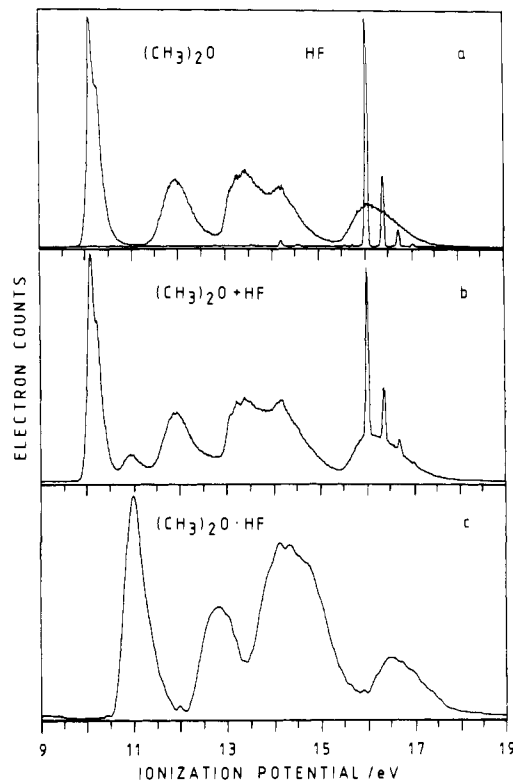


Figure 2. He I photoelectron spectra of (a) $(\text{CH}_3)_2\text{O}$ and HF, (b) a mixture of $(\text{CH}_3)_2\text{O}$ and HF showing the presence of the complex $(\text{CH}_3)_2\text{O}\cdot\text{HF}$, and (c) the complex $(\text{CH}_3)_2\text{O}\cdot\text{HF}$ obtained by spectrum stripping.

On the assumption that the weak band near 11 eV in Figure 2b is the first PE band of the complex $(\text{CH}_3)_2\text{O}\cdot\text{HF}$, the spectrum stripping of the $(\text{CH}_3)_2\text{O}$ and HF shown in Figure 2a from the mixed spectrum of Figure 2b is fairly straightforward. The resulting stripped spectrum is relatively noisy but smoothing with a Gaussian function of 5 point halfwidth gives the spectrum of Figure 2c. This is assigned as that of the $(\text{CH}_3)_2\text{O}\cdot\text{HF}$ complex, and clearly shows the 11 eV first band as well as prominent higher IP bands near 13 and 14 eV consistent with the intensity enhancement described earlier. These bands and a further one at 16.5 eV clearly represent $(\text{CH}_3)_2\text{O}$ bands moved to higher IPs on complex formation.

However, the bands of the complex in the 13.5–15.0-eV region are relatively more intense than those in the monomer $(\text{CH}_3)_2\text{O}$. The overlapping bands which cause this arise from the HF moiety in the complex being the HF π band shifted to lower IP and with a generally structureless profile.

At room temperature the vapor pressure of $(\text{CH}_3)_2\text{S}$ is lower than that of HF so that mixtures used with the effusive nozzle have maximum stagnation pressures of only ~ 0.2 atm. Despite the expected weaker nature of the $(\text{CH}_3)_2\text{S}\cdot\text{HF}$ complex, the expected first band of the complex at a higher IP than the $(\text{CH}_3)_2\text{S}$ first band can be seen in the time-averaged spectrum of Figure 3b which is that of a $(\text{CH}_3)_2\text{S}/\text{HF}$ mixture containing an excess of HF. The monomer spectra are shown in Figure 3a, and when these are stripped from the mixed spectrum the resulting spectrum after Gaussian smoothing is that of Figure 3c. Because this spectrum shows the upward IP shifts anticipated for the $(\text{CH}_3)_2\text{S}$ -based bands of the complex together with intense bands in the 15-eV region which can be regarded as the downward IP shifted HF π band, this is assigned as the He I spectrum of the $(\text{CH}_3)_2\text{S}\cdot\text{HF}$ complex.

Calculations and Discussion

The intermolecular complexes $(\text{CH}_3)_2\text{O}\cdot\text{HF}$ and $(\text{CH}_3)_2\text{S}\cdot\text{HF}$ have not been the object of intensive theoretical study to date. The only extensive data in the recent literature are the Gaussian basis SCF-MO calculations by Hincliffe¹⁴ of the equilibrium geometry and electron distribution of $(\text{CH}_3)_2\text{O}\cdot\text{HF}$. These calculations, carried out for essentially planar structures, showed that

(13) E. Nagy-Felsobuki and J. B. Peel, *J. Electron Spectrosc. Relat. Phenom.*, **15**, 61 (1979).

(14) A. Hincliffe, *Adv. Mol. Relaxation Interact. Processes*, **13**, 309 (1978).

(12) G. D. Willett, Ph.D. Thesis, La Trobe University, 1977.

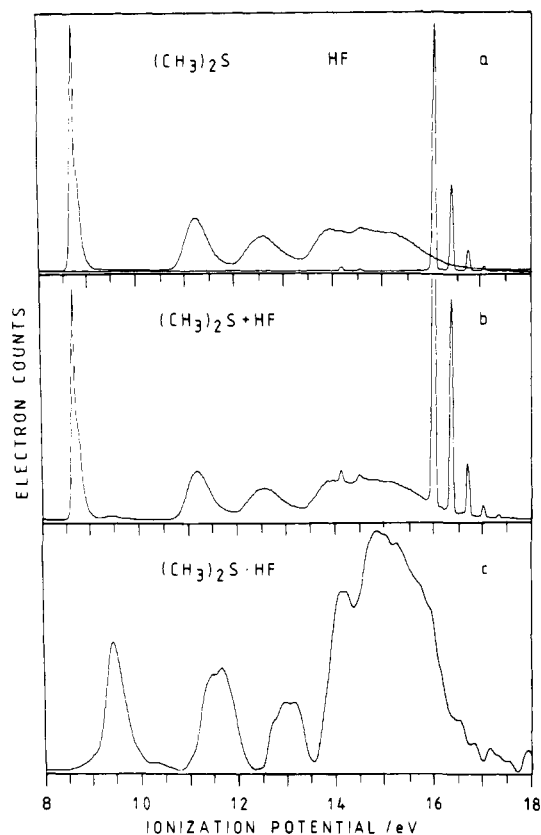


Figure 3. He I photoelectron spectra of (a) $(\text{CH}_3)_2\text{S}$ and HF, (b) a mixture of $(\text{CH}_3)_2\text{S}$ and HF showing the presence of the complex $(\text{CH}_3)_2\text{S}\cdot\text{HF}$, and (c) the complex $(\text{CH}_3)_2\text{S}\cdot\text{HF}$ obtained by spectrum stripping.

both the equilibrium hydrogen bond length, $R(\text{O}\cdots\text{H})$, and the hydrogen bond energy, ΔU , of the complex are basis set dependent.

Our earlier SCF-MO calculations on $(\text{CH}_3)_2\text{O}\cdot\text{HCl}$ suggested a nonplanar geometry for this complex. When a similar augmented STO-3G* basis was used for calculations on $(\text{CH}_3)_2\text{O}\cdot\text{HF}$ and $(\text{CH}_3)_2\text{S}\cdot\text{HF}$ the minimum energy geometries obtained were planar for $(\text{CH}_3)_2\text{O}\cdot\text{HF}$ but nonplanar for $(\text{CH}_3)_2\text{S}\cdot\text{HF}$, the energy minimum in the latter occurring at an out-of-plane angle of 67° made by the S-H-F line with the C-S-C plane.

The augmented STO-3G* basis consisted of Pople's STO-3G minimum basis¹⁵ with additional 1s, 2s, and 2p STOs on fluorine each of exponent 1.5. The effect of this extension is to correct for the poorer performance of the minimum basis set for HF compared with $(\text{CH}_3)_2\text{O}$ and $(\text{CH}_3)_2\text{S}$. When the Koopmans approximation is used the STO-3G basis underestimates the $(\text{CH}_3)_2\text{O}$ IPs by a mean of 0.4 eV and the HF IPs by a mean of 3.6 eV. By contrast, the STO-3G* basis reduces this difference to 0.5 eV for HF. Consequently, there is a good correlation between calculated and experimental IPs for the monomers considered together when the augmented basis is used. This is also the case for $(\text{CH}_3)_2\text{S}$ and HF considered together. This means that calculations using the augmented STO-3G* basis for the respective complexes should show improved correlations with their experimental IP data.

While the Koopmans IPs from the STO-3G calculations are low by up to 1 eV for $(\text{CH}_3)_2\text{O}$ and up to 2 eV for $(\text{CH}_3)_2\text{S}$, the 4-31G basis calculations using the -0.9 scale factor give generally better quantitative agreement between experimental and calculated IPs. However, the correlations between these are poorer than those for the STO-3G basis.

The 4-31G basis gives similar minimum-energy geometries to the STO-3G* basis in respect to the planarity of $(\text{CH}_3)_2\text{O}\cdot\text{HF}$ and the nonplanar result for $(\text{CH}_3)_2\text{S}\cdot\text{HF}$. However, with the

Table I. Comparison of Calculated and Experimental Vertical Ionization Potentials (eV) of $(\text{CH}_3)_2\text{O}\cdot\text{HF}$ and $(\text{CH}_3)_2\text{S}\cdot\text{HF}$

$(\text{CH}_3)_2\text{O}\cdot\text{HF}$				
exptl ^a	assignment MO (C_{2v})	STO-3G* (-e)	4-31G (-0.9e)	ext. basis ^b (-0.9e)
11.04	3b ₁ (n_{O})	10.24	11.19	11.04
12.92	9a ₁ (\bar{n}_{O})	11.83	12.49	12.53
14.2	5b ₂ (π_{CH_3})	13.91	13.54	13.50
14.4	2b ₁	14.25	13.81	14.63
14.4	4b ₂ (π_{F})	14.25	13.81	14.64
14.7	1a ₂ (π_{CH_3})	14.83	14.14	14.07
16.5	3b ₂ (σ_{CO})	16.57	16.35	16.35
16.9	8a ₁ (π_{CH_3})	16.85	16.01	16.13
17.3	1b ₁ (π_{CH_3})	17.53	16.98	16.78
18.1	7a ₁ (σ_{HF})	18.44	17.53	17.99
$(\text{CH}_3)_2\text{S}\cdot\text{HF}$				
exptl ^a	assignment MO (C_s)	STO-3G* (-e)	4-31G (-0.9e)	
9.5	15a' (n_{S})	7.62	8.98	
11.6	14a' (σ_{CS})	10.27	11.05	
13.0	7a'' (σ_{CS})	12.13	12.40	
14.1	6a'' (π_{CH_3})	14.75	14.33	
14.8	13a' (π_{F})	14.78	14.44	
14.8	5a'' (π_{F})	14.79	14.44	
15.2	4a'' (π_{CH_3})	15.07	14.70	
15.7	12a' (π_{CH_3})	15.72	15.32	
15.7	11a' (π_{CH_3})	15.79	15.35	
	10a' (σ_{HF})	18.43	17.22	

^a Accuracies vary between ± 0.05 and ± 0.2 eV. ^b From ref 14.

respective monomer species held at their experimental geometries, the intermolecular equilibrium $R(\text{O}\cdots\text{H})$ and $R(\text{S}\cdots\text{H})$ distances vary with the basis set. In going from the STO-3G* to the 4-31G basis the $R(\text{O}\cdots\text{H})$ distance in $(\text{CH}_3)_2\text{O}\cdot\text{HF}$ decreases from 1.72 to 1.67 Å, the corresponding hydrogen bond energies being calculated as 60 and 57 kJ mol⁻¹, respectively. These are in line with Hinchliffe's results and illustrate his observation¹⁴ that the low quality of the basis sets used is responsible for an underestimation of the intermolecular bond distance. For $R(\text{S}\cdots\text{H})$ in $(\text{CH}_3)_2\text{S}\cdot\text{HF}$ the calculated equilibrium values are 2.26 and 2.34 Å respectively for the STO-3G* and 4-31G basis sets, with corresponding hydrogen bond energies of 36 and 32 kJ mol⁻¹.

The assignment of the experimental vertical IPs of each complex given in Table I assumes the ordering suggested by the Koopmans approximation applied to the calculated eigenvalues. Because of the considerable overlapping of bands in specific regions of each spectrum, the precise ordering of particular states must be regarded as uncertain. This is obviously the case for the higher IP bands of the $(\text{CH}_3)_2\text{O}$ monomer, so that assignment of the $(\text{CH}_3)_2\text{O}\cdot\text{HF}$ complex must at least reflect this uncertainty. The localized orbital description indicated in Table I is based on the LCAO coefficients which show that there is very little mixing of monomer MOs in forming the complex. The description of the $(\text{CH}_3)_2\text{O}$ -based MOs is in agreement with the localized orbitals listed by Kimura et al.¹⁶ An apparent disagreement with the description of Jorgensen and Salem¹⁷ in the case of the 3b₂ and 5b₂ MOs arises because both are actually mixtures of both π_{CH_3} and σ_{CO} character.

However, it is possible to estimate the location of the π_{F} bands with reasonable accuracy by comparing the spectra of monomer and complex. For $(\text{CH}_3)_2\text{O}\cdot\text{HF}$ the overlapping band between 13.5 and 15.5 eV must include those arising from the 13.0-15.0-eV bands of the $(\text{CH}_3)_2\text{O}$ monomer shifted to higher IP. Because these bands in $(\text{CH}_3)_2\text{O}$ show a trough between two maxima, the loss of this trough in the complex suggests that the π_{F} bands occupy the central section of this region and are hence assigned at 14.4 eV.

(16) K. Kimura, S. Katsumata, Y. Achiba, T. Yamazaki, and S. Iwata, in "Handbook of He I Photoelectron Spectra of Fundamental Organic Molecules", Japan Scientific Societies Press, Tokyo, 1981.

(17) W. L. Jorgensen and L. Salem, in "The Organic Chemists Book of Orbitals", Academic Press, New York, 1973.

(15) W. J. Hehre, R. F. Stewart, and J. A. Pople, *J. Chem. Phys.*, **51**, 2657 (1969).

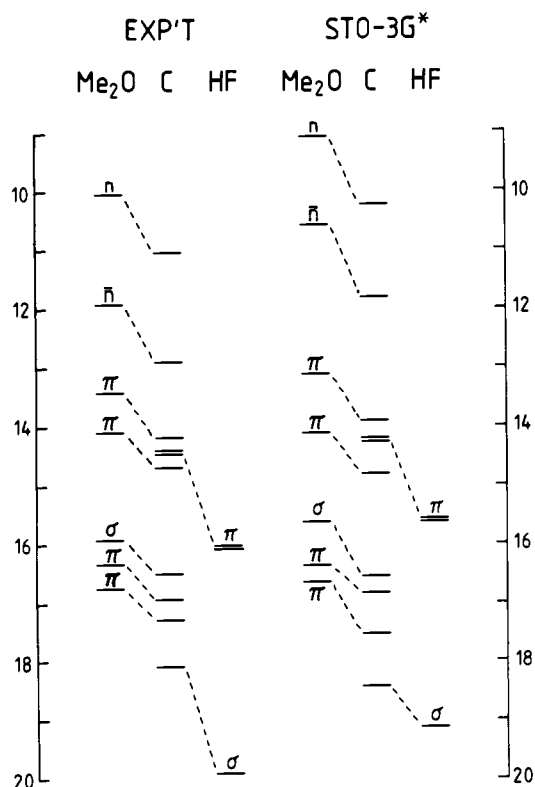


Figure 4. Correlation diagrams of the vertical ionization potentials (eV) of the monomers and complex of $(\text{CH}_3)_2\text{O}\cdot\text{HF}$. The experimental values are compared with theoretical data from the STO-3G* basis calculations. For $(\text{CH}_3)_2\text{O}$ the π and σ ionizations are referred to in the text as π_{CH_3} and σ_{CO} .

Similarly a comparison of the $(\text{CH}_3)_2\text{S}$ and $(\text{CH}_3)_2\text{S}\cdot\text{HF}$ spectra suggests that the relatively high intensity around 15 eV in the spectrum of the complex can only be associated with the π_{F} states of HF shifted to lower IP. As indicated in Table I, these IP assignments might only be regarded as accurate to within about ± 0.2 eV.

The Koopmans IPs from the STO-3G* and 4-31G calculations, given in Table I, show a pattern in good general agreement with the experimental data. The Dunning basis eigenvalues obtained by Hincliffe and scaled by -0.9 are also listed for $(\text{CH}_3)_2\text{O}\cdot\text{HF}$. The differences between these extended basis eigenvalues and our 4-31G results are seen to be essentially for the orbitals of HF, indicating that the main improvement represented by the extended basis is for the F atom basis.

The effects of complexation are shown better by comparisons of monomer and dimer IPs as illustrated in the appropriate correlation diagrams of Figures 4 and 5. These separately compare the experimental IPs and the STO-3G* theoretical IPs.

It is interesting to compare the experimental IP shifts occurring on the complexation of $(\text{CH}_3)_2\text{O}$ and $(\text{CH}_3)_2\text{S}$ by HF with the data obtained earlier for $(\text{CH}_3)_2\text{O}\cdot\text{HCl}$. These are listed for the three complexes in Table II. While the n_0 and n_s shifts are measured accurately, the shifts assigned to π_{CH_3} and \bar{n}_0 , σ_{CO} , or σ_{CS} are only approximate in that both the identification and assignment of the bands in the spectra of the complexes are not clearly established. The π_{F} and π_{Cl} shifts are obtained with reasonable accuracy.

On the basis of ab initio SCF-MO calculations Umeyama and Morokuma¹⁸ have concluded that "normal" hydrogen bonded complexes, such as those of the present study, are characterized by intermolecular bonding which is strongly electrostatic in nature, with a small but significant contribution of charge transfer. Our calculations show that, in agreement with the data obtained by Hincliffe¹⁴ and the studies on related complexes by Morokuma

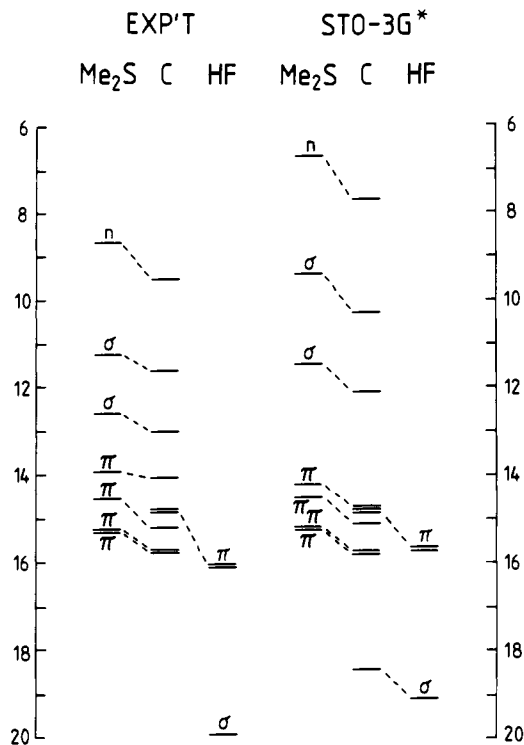


Figure 5. Correlation diagrams of the vertical ionization potentials (eV) of the monomers and complex of $(\text{CH}_3)_2\text{S}\cdot\text{HF}$. The experimental values are compared with theoretical data from the STO-3G* basis calculations. For $(\text{CH}_3)_2\text{S}$ the π and σ ionizations are referred to in the text as π_{CH_3} and σ_{CS} .

Table II. Comparison of Experimental Ionization-Potential Shifts^a (eV) and Calculated Dipole-Induced Potential-Energy Shifts (in Parentheses); Calculated Charge-Transfer (CT) and Electronic-Relaxation (ER) Shifts for the π Ionizations

	$(\text{CH}_3)_2\text{O}\cdot\text{HF}^b$	$(\text{CH}_3)_2\text{S}\cdot\text{HF}^c$	$(\text{CH}_3)_2\text{O}\cdot\text{HCl}^{d,e}$
n_0 or n_s	1.0 (1.02)	0.8 (0.89)	0.6 (0.85)
π_{CH_3}	0.6 (0.61)	0.3 (0.38)	0.4 (0.53)
\bar{n}_0 , σ_{CO} , or σ_{CS}	0.8 (0.97)	0.3 (0.63)	0.5 (0.75)
π_{F} or π_{Cl}	-1.6 (-0.56)	-1.2 (-0.23)	-1.0 (-0.34)
	(-0.32) _{CT}	(-0.35) _{CT}	(-0.17) _{CT}
	(-0.24) _{ER}	(-0.35) _{ER}	(-0.17) _{ER}

^a IP (complex) - IP (monomer). ^b Using $R(\text{O-H}) = 1.72$ Å and planar geometry. ^c Using $R(\text{S-H}) = 2.26$ Å and an out-of-plane angle of 67° . ^d Using $R(\text{O-H}) = 1.9$ Å and an out-of-plane angle of 34° . ^e Data from ref 8.

et al.,¹⁹ complexation results in a redistribution of charge density according to $\text{R}^{\delta+}-\text{Y}^{\delta-} \cdots \text{H}^{\delta+}-\text{X}^{\delta-}$ with both monomeric units increasing in polarity together with a small net electron transfer from RY to HX.

Since any increase of electron density on O (or S) would cause a decrease in IP of n_0 (or n_s), the observed increase in these IPs on complexation is clearly due to a dominant electrostatic effect arising from the approach of the polar HF moiety. A through-space dipole-induced potential-energy shift can be calculated by using the decomposition scheme for molecular interactions proposed by Kitaura and Morokuma²⁰ with the SCF-MO calculations. This provides a set of constrained wave functions of the intermolecular complex such that electrostatic, exchange, polarization, charge-transfer, and other effects are separately analyzed. The electrostatic component of each calculated IP shift is compared with the experimental value in Table II. The generally good agreement between the experimental and calculated data for the

(19) M. Tsuda, H. Touhara, K. Nakanishi, K. Kitaura, and K. Morokuma, *J. Am. Chem. Soc.*, **100**, 7189 (1978).

(20) K. Kitaura and K. Morokuma, *Int. J. Quantum Chem.*, **10**, 325 (1976).

(18) H. Umeyama and K. Morokuma, *J. Am. Chem. Soc.*, **99**, 1316 (1977).

(CH₃)₂O and (CH₃)₂S moieties indicates that the electrostatic effect of the complexed HF or HCl moiety is the dominant influence in increasing the monomer IPs on complexation. These calculations are described in more detail elsewhere.²¹

However, the π_F and π_{Cl} IP shifts are larger than any measured for (CH₃)₂O and (CH₃)₂S and the through-space dipole-induced potential-energy term only accounts for a fraction of the observed IP shifts in each case. The remaining amounts are accounted for by the effects of charge transfer and electronic relaxation. The decomposition scheme allows the calculation of the IP shift associated with charge transfer; the resulting values are labeled CT in Table II.

Molecular open-shell calculations are required to obtain theoretical estimates of electronic-relaxation effects associated with ionization. The data obtained for total ion energies of the appropriate valence-hole states of the monomer and complexed HF⁺ and HCl⁺ species allow the calculation of the differences in relaxation energies which represent the electronic-relaxation contribution to IP shift. The calculations which are described in more detail elsewhere²¹ give the results labeled ER in Table II. These indicate that both charge-transfer and electronic-relaxation effects contribute comparable amounts to the π_F and π_{Cl} IP shifts on complexation. The calculated charge transfers involved are only small, being 0.06 e from (CH₃)₂O to HF, 0.05 e from (CH₃)₂S to HF, and 0.05 e from (CH₃)₂O to HCl. The electronic-relaxation effect involves the highly polarizable (CH₃)₂O or (CH₃)₂S moieties in each complex, acting as a source of electron density which considerably stabilizes the localized valence hole in HF⁺

or HCl⁺. The calculations show that the movement of electron density is 0.13 e to HF⁺ in (CH₃)₂O·HF⁺, 0.16 e to HF⁺ in (CH₃)₂S·HF⁺, and 0.11 e to HCl⁺ in (CH₃)₂O·HCl⁺.

Conclusion

On the basis of the He I photoelectron spectra measured for (CH₃)₂O·HF and (CH₃)₂O·HCl, the much weaker gas-phase complex (CH₃)₂S·HF has been identified by its He I spectrum. The ionization-potential shifts associated with complexation are shown to arise from the electrostatic effect of the polar HF moiety on the (CH₃)₂O and (CH₃)₂S orbitals, but charge transfer accompanying complexation and electronic relaxation accompanying ionization are mainly responsible for the decreased IPs associated with its nonbonding π_F electrons. The neglect of electronic-relaxation effects is seen to have no influence on the spectral assignment based on the Koopmans approximation and the closed-shell wave functions.

This study provides a definitive spectroscopic identification of the (CH₃)₂S·HF species and indicates the considerable power of the photoelectron technique in the study of molecular systems of limited accessibility.

Acknowledgment. This work was supported by the Australian Research Grants Scheme. We acknowledge the La Trobe Postgraduate Award held by F.C. and the Commonwealth Postgraduate Award held by M.K.L. and are grateful for generous allocations of computing time by the La Trobe University Computer Centre.

Registry No. Dimethyl ether, 115-10-6; dimethyl sulfide, 75-18-3; hydrogen fluoride, 7664-39-3.

(21) J. B. Peel, *Aust. J. Phys.*, in press.

Intermediates in the Sulfide Reduction of the 3,5-Diphenyl-1,2-dithiolylium Cation: A Resonance Raman Study

Olavi Siiman,*[†] Sujin Shobsngob,[†] and James Fresco[†]

Contribution from the Departments of Chemistry, Clarkson College of Technology, Potsdam, New York 13676, and McGill University, Montreal, Quebec H3A 2K6, Canada. Received February 12, 1982

Abstract: Resonance Raman spectra of two intermediates, absorbing at 545 and 473 nm, in the reaction between 3,5-diphenyl-1,2-dithiolylium perchlorate and excess sodium sulfide in ethanolic solution have been measured. Both chromophoric intermediates are assigned to anionic structures of the dithio- β -diketonate by using similar spectra of the disulfide cation and bis(dithiodibenzoylmethane)nickel(II) for comparison. The shorter lived transient is tentatively assigned to an open-chain disulfide anion or to the *cis*-S,S isomer of the dithio anion. The longer lived species is assigned to a *trans* isomer of the anion. Intense resonance Raman bands at 1140, 733, 550, and 380 cm⁻¹ were assigned to $\nu(C-Ph) + \nu(C-S)$, $\nu(C-S)$, $\delta(CCC) + \delta(CCS)$, and $\delta(C-S)$ vibrational modes in the intermediates. A medium-strong band at 600 cm⁻¹ was linked with the open-chain $\nu(S-S)$ mode or $\delta(CCS)$ and $\delta(CCC)$ modes.

In the mechanism of disulfide bond reduction of straight-chain organic disulfides with sulfide ion, it has been postulated¹ that 1 mol of thiolate and 1 mol of organic persulfide are formed with subsequent loss of sulfur in the persulfide, S₂²⁻, ion form. In similar reactions of cyclic disulfide cations, it has been suggested² that persulfide formation is preceded by nucleophilic attack on the 3- or 5-ring-carbon position of the 3,5-diphenyl-1,2-dithiolylium cation, hereafter denoted by 3,5-Ph₂D⁺, to form an adduct between cation and anionic nucleophile. The electronic absorption spectra of several intermediates in the conversion of the 3,5-diphenyl-

1,2-dithiolylium cation to monothiodibenzoylmethane have recently been measured.³ The reaction between disulfide cation and sodium sulfide in aqueous or alcoholic media is of particular interest since an expected intermediate is the dithiodibenzoylmethane anion. The existence of the ligand⁴ has been implied as a result of trapping its metal complexes and spectroelectrochemical studies⁵ of the disulfide cation reduction. To identify

(1) Rao, G. S.; Gorin, G. *J. Org. Chem.* 1959, 24, 749.

(2) Leaver, D.; McKinnon, D. M.; Robertson, W. A. H. *J. Chem. Soc.* 1965, 32.

(3) Shobsngob, S.; Fresco, J. *Can. J. Spectrosc.* in press.

(4) Lockyer, T. N.; Martin, R. L. *Prog. Inorg. Chem.* 1980, 27, 223.

[†] Clarkson College of Technology.

[†] McGill University.